

Immobilization of **1–3** on the transducer surface: The surface of the glass is cleaned with a freshly prepared Piranha solution ($\text{H}_2\text{SO}_4/\text{H}_2\text{O}$ 2/1) (1 h), washed with water, and dried at room temperature (RT). The silanization takes place with a solution of 3-glycidioxypropyltrimethoxysilane (20% in toluene; 4 h at 110 °C). To link the cyclopeptides to the surface, a solution of **1**, **2**, or **3** (0.1 mg mL⁻¹) in phosphate buffer (50 mM, pH 8) is added (24 h, RT). Then it is washed with brine (1M) and water. To characterize the cyclopeptide-functionalized glass supports, static contact-angle measurements were carried out with six different solvents and the polar (σ^p) and disperse share (σ^d) in the surface energy were determined. Immobilized cyclopeptide **1**: $\sigma^d = 23.51 \text{ mN m}^{-1}$, $\sigma^p = 21.37 \text{ mN m}^{-1}$. Immobilized cyclopeptide **2**: $\sigma^d = 23.18 \text{ mN m}^{-1}$, $\sigma^p = 23.49 \text{ mN m}^{-1}$. Immobilized cyclopeptide **3**: $\sigma^d = 23.27 \text{ mN m}^{-1}$, $\sigma^p = 25.63 \text{ mN m}^{-1}$.

Received: June 24, 1998 [Z 12041 IE]
German version: *Angew. Chem.* **1998**, *110*, 3503–3505

Keywords: chemosensors • cyclopeptides • interference spectroscopy • combinatorial chemistry • molecular recognition

- [1] M. F. Cristofaro, A. R. Chamberlin, *J. Am. Chem. Soc.* **1994**, *116*, 5089–5098.
- [2] X. X. Zhang, J. S. Bradshaw, R. M. Izatt, *Chem. Rev.* **1997**, *97*, 3313–3361.
- [3] W. C. Still, *Acc. Chem. Res.* **1996**, *29*, 155–163.
- [4] M. M. Conn, J. Rebek, Jr., *Chem. Rev.* **1997**, *97*, 1647–1668.
- [5] C. M. Deber, E. R. Blout, *J. Am. Chem. Soc.* **1974**, *96*, 7566–7568.
- [6] a) H. Miyake, Y. Kojima, *Coord. Chem. Rev.* **1996**, *148*, 301–314; b) H. Kataoka, T. Hanawa, T. Katagi, *Chem. Pharm. Bull.* **1992**, *40*, 570–574.
- [7] F. Wudl, F. J. Gaeta, *J. Chem. Soc. Chem. Commun.* **1972**, 107.
- [8] G. Jung, H. Hofstetter, S. Feiertag, D. Stoll, O. Hofstetter, K.-H. Wiesmüller, V. Schurig, *Angew. Chem.* **1996**, *108*, 2261–2262; *Angew. Chem. Int. Ed. Engl.* **1996**, *35*, 2148–2150.
- [9] *Combinatorial Peptide and Nonpeptide Libraries* (Ed.: G. Jung), VCH, Weinheim, **1996**.
- [10] H. Kessler, R. Gratias, G. Hessler, M. Gurrath, G. Müller, *Pure Appl. Chem.* **1996**, *68*, 1201–1205.
- [11] G. Gauglitz, A. Brecht, G. Kraus, W. Nahm, *Sens. Actuators B* **1993**, *11*, 21–27.
- [12] A. Brecht, J. Piehler, G. Lang, G. Gauglitz, *Anal. Chim. Acta* **1995**, *311*, 289–300.
- [13] D. W. Armstrong, D. Rundlett, J.-R. Chen, *Chirality* **1994**, *6*, 496–509.
- [14] *Comprehensive Polymer Science, Polymer Properties*, Pergamon, Oxford, **1989**.

FT-IR Mapping—A New Tool for Spatially Resolved Characterization of Polymer-Bound Combinatorial Compound Libraries with IR Microscopy**

Wolfgang J. Haap,* Tilmann B. Walk, and Günther Jung*

A decisive advantage of combinatorial organic solid-phase chemistry^[1–5] for finding lead structures is its higher throughput compared to previous synthetic methods, as easily automated reactions are preferentially carried out on polymer resins.^[6] Further improvement of the efficiency is directed to an increasing miniaturization of the synthesis as well as screening of the prepared compounds. Resin-bead analysis plays an important role in the development of such technologies. With the techniques that have now been established for analyzing single resin beads—such as NMR spectroscopy,^[7, 8] matrix-assisted laser desorption ionization time-of-flight (MALDI-TOF) mass spectrometry, and FT-IR microscopy^[9–11]—only polymer-bound single compounds could be analyzed so far. In combinatorial chemistry, however, techniques are needed with which a large number of compounds can be analyzed simultaneously.

Owing to its high sensitivity, the simplicity of the apparatus, and the high sample throughput, IR microscopy is suited for parallel analysis. The combination of a FT-IR microscope with a motor-driven *x-y* stage allows the automatic spectral mapping of surfaces and objects embedded in them. If single resin beads are embedded in a KBr window by pressing, they can be visualized with this measuring arrangement in the form of an IR map. The superpositioning of the visible video image of several resin beads with the corresponding IR map (Figure 1) shows the good correlation of both types of representations. In this case, for the IR reconstruction the typical polystyrene combination vibration at 1942 cm⁻¹ was chosen.

Through mapping of larger areas, hundreds of embedded resin beads can be detected and the compounds bound to them identified. To exhibit the potential of this method, a model library of isoxazolidines^[12] on Rink amide ARAM resin was synthesized by the split-and-combine method^[13] (Scheme 1). The polymer-bound library obtained consists of a total of 18 compounds. If one considers the different building blocks of the synthesis, a nitro group or the carboxamidomethyl residue is found in 50% each of the

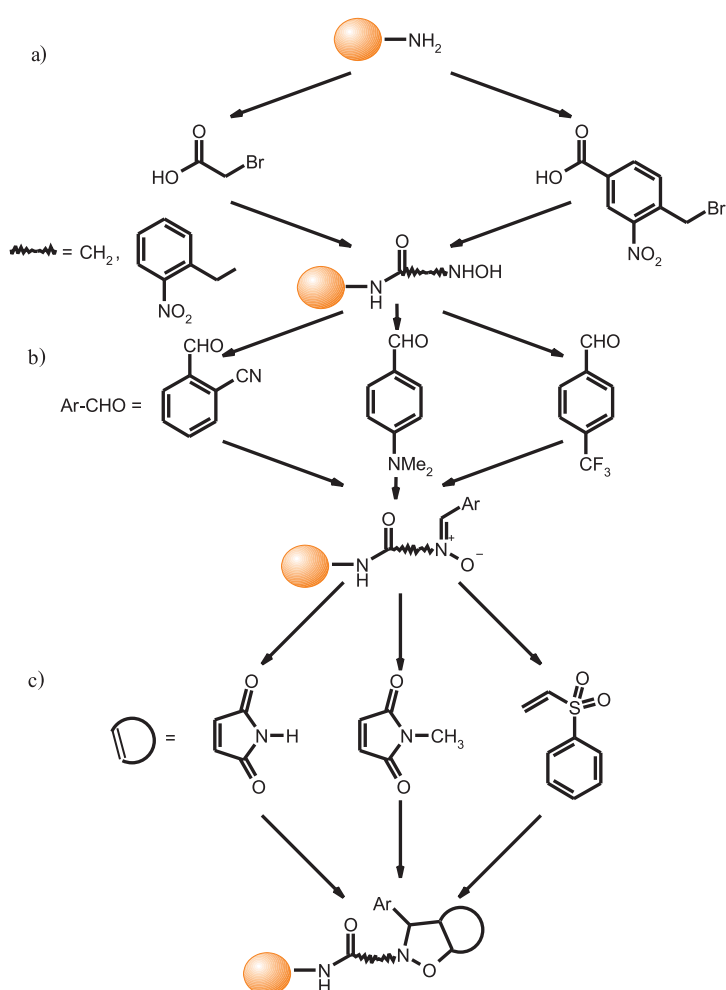
[*] Dr. W. J. Haap,^[+] Prof. Dr. G. Jung, Dipl.-Chem. T. B. Walk
Institut für Organische Chemie der Universität
Auf der Morgenstelle 18, D-72076 Tübingen (Germany)
Fax: (+49) 7071-296925
E-mail: guenther.jung@uni-tuebingen.de

[+] New address:
Ciba Speciality Chemicals Inc., BS Antimicrobials
P.O. Box 1266, D-79630, Grenzach-Wyhlen (Germany)
E-mail: wolfgang.haap@cibasc.com

[**] This work was supported by the Bundesministerium für Bildung, Forschung und Technologie BMBF (FKZ 0311000; Librarian II, Teilprojekt "Kombinatorische Chemie und Synthesemonitoring"). We thank Dr. A. Rager (Bruker, Karlsruhe, Germany) for the technical assistance.



Figure 1. UV/Vis video image and IR reconstruction of four polystyrene resin beads with a diameter of about 80 μm . The IR map was obtained with a motor-driven x - y stage in combination with an IR microscope. For the reconstruction of the resin beads the integral of the polystyrene combination vibration at 1942 cm^{-1} was used.



Scheme 1. Solid-phase synthesis of isoxazolidines according to the split-and-combine method. a) Distribution of the resin into two equal portions, coupling of bromocarboxylic acids with N,N' -diisopropylcarbodiimide (DIC), combination of the resin, substitution with hydroxylamine; b) distribution of the resin into three equal portions, condensation with three different aromatic aldehydes to the corresponding nitrones, combination of the resin; c) distribution of the resin into three equal portions, cycloaddition with three different dipolarophiles to isoxazolidines, combination of the resin.

compounds; a cyano, N,N -dimethylamino, or trifluoromethyl group in 33 % each; and a succinimide, N -methylsuccinimide, or sulfone group in 33 % each. To verify that this library was successfully synthesized, a portion of the resin was removed, and the compounds were cleaved from the polymer with trifluoroacetic acid and analyzed with HPLC electrospray ionization mass spectrometry. All the compounds shown could be identified. Upon cycloaddition of the maleimides *endo/exo* isomers and, in the case of the vinylsulfones, regioisomers were obtained. This led to complex chromatograms of isomer compound mixtures; coelution occurred often. A quantification of the single compounds is not possible, and the peak area in the UV trace (detection at 214 nm) did not correlate with those of the total ion current chromatogram in the mass spectrum.

The isoxazolidine library prepared according to Scheme 1 was embedded in a KBr window by pressing. An area of $3 \times 3\text{ mm}^2$ was automatically mapped. When the polystyrene absorption at 1942 cm^{-1} was used to visualize the IR map, all resin beads contained on the surface were detected (Figure 2).

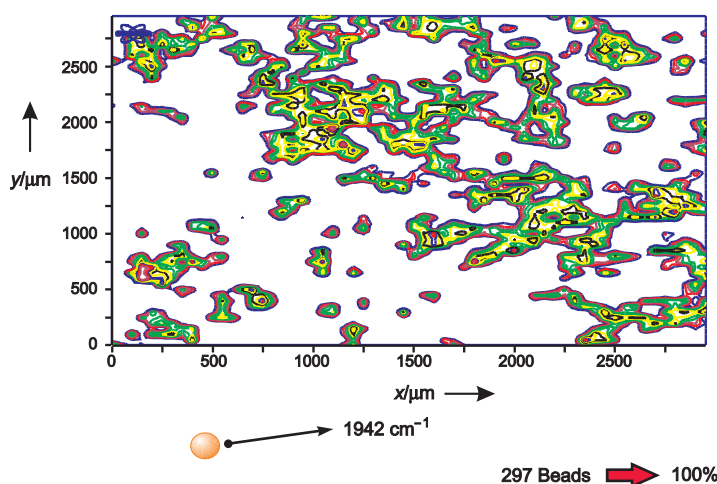


Figure 2. IR map of an area ($3 \times 3\text{ mm}^2$) of a KBr window in which resin beads of the isoxazolidine library are embedded. By application of the polystyrene absorption at 1942 cm^{-1} all resin beads were detected. White region: KBr window; colored region: resin beads. There are a total of 297 resin beads in the scanned area.

Through choice of different absorption bands for visualization, those resin beads carrying a specific functional group can be selectively “fished out” from this library of 297 resin beads. For example, the resin beads with the N -methylsuccinimide group are extracted spectroscopically from the resin-bead mixture by visualization by means of the carbonyl absorption at 1715 cm^{-1} . In the scanned area there are a total of 112 resin beads (39.1%) with this functional group (Figure 3). Analogous IR maps could be obtained for further functional groups (Figure 4).

The IR analysis of polymer-bound molecules is made difficult by the strong absorption of the polymer matrix itself. In the IR spectrum containing polymer and anchor absorptions, for example, signals for neither the N,N -dimethylamino nor the carboxamidomethyl groups can be recognized. However, as all further functional groups can be clearly differ-

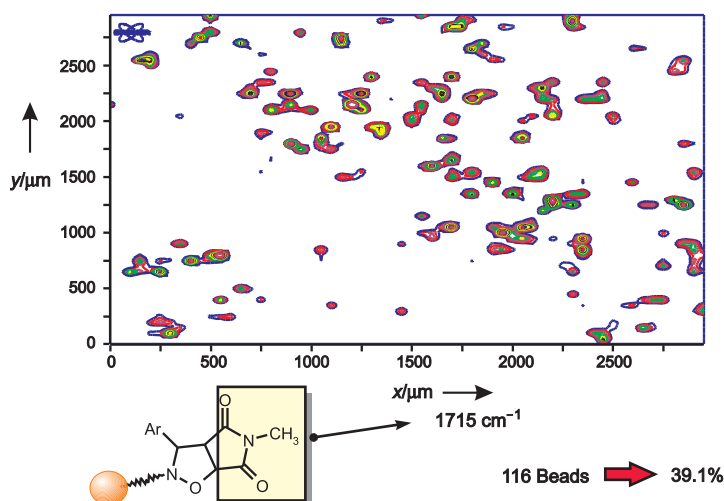


Figure 3. “*N*-Methylsuccinimide” resin beads extracted from the library by visualization over the carbonyl absorption at 1715 cm^{-1} .

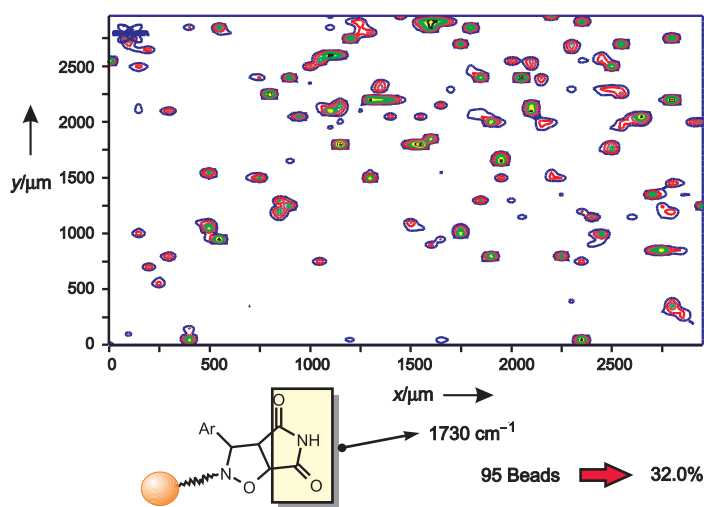


Figure 4. “Succinimide” resin beads extracted from the library by visualization over the carbonyl absorption at 1730 cm^{-1} .

entiated from one another, the number of resin beads carrying a specific group is given by the exclusion principle. If this method is applied to all resin beads, the distribution of all functional groups can be determined by single counting of the resin beads by data processing programs (Table 1).

Despite the relatively small amount of resin beads in the scanned regions, no significant deviations from the expected statistical distribution of the individual functional groups are observed. Although the carboxamidomethyl, cyano, and *N*-methylimide groups are somewhat overrepresented, their contributions are on the same order of magnitude. When applied together with a LC-MS analysis, IR mapping allows a statistical investigation and thus a rapid quality control of the library synthesized by the split-and-combine method.

The decisive advantage of this technique is that IR analysis, in contrast to mass spectrometry, can be carried out without destruction of the sample and with spatial resolution. Furthermore, a direct identification of resin-bound molecules is possible through superpositioning of the IR maps. If, for example, the maps of the imide (1730 cm^{-1}), nitro

Table 1. Statistical distribution [%] (the theoretical values are given in parentheses) of resin beads with specific functional groups.

	32.0 (33.3)		41.4 (50)		42.4 (33.3)
	39.1 (33.3)		58.6 (50)		32.3 (33.3)
	28.9 (33.3)				25.3 (33.3)

(1360 cm^{-1}), and cyano absorptions (2225 cm^{-1}) are placed on top of each other, the resin beads that carry exclusively compound **1** can be identified with spatial resolution in the overlapping regions (stars in Figure 5) of the functional groups. The FT-IR spectra of the individual resin beads extracted from the maps clearly confirm attachment of **1** to the resin bead (Figure 6).

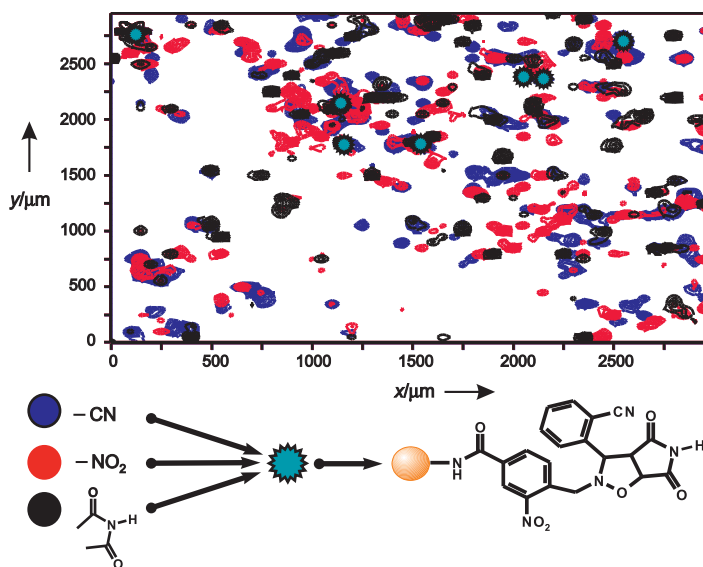


Figure 5. “FT-IR tagging” by superpositioning of the IR maps of imide (1730 cm^{-1}), nitro (1360 cm^{-1}), and cyano absorptions (2225 cm^{-1}). Resin beads on which **1** is immobilized were identified through overlapping regions of all IR maps.

In summary, a method has been developed that allows the spatially resolved and destruction-free characterization and quality control of polymer-bound compound libraries. Furthermore, by superpositioning of different IR maps, compounds immobilized on individual resin beads can be identified. Through improved embedding techniques, even larger areas with many resin beads can be mapped very quickly. This

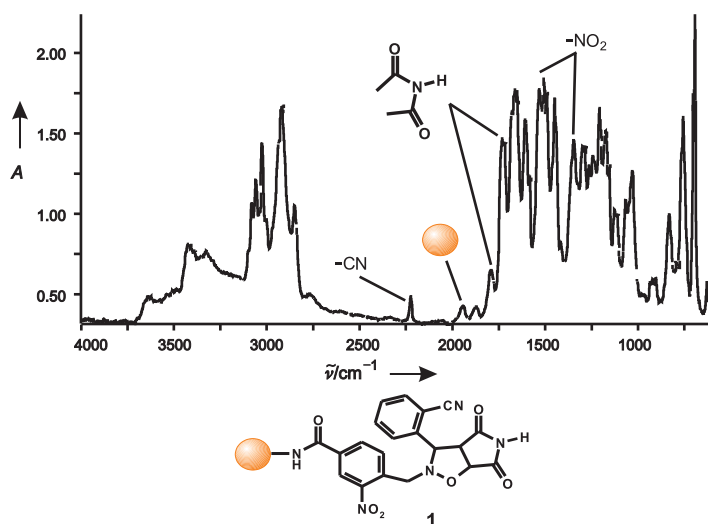


Figure 6. FT-IR spectrum of an individual resin bead on which **1** is immobilized.

method can thus provide a valuable contribution to the development of miniaturized syntheses on individual resin beads. The combination of IR mapping with MS and HPLC-MS analysis means that tagging concepts can be abandoned; technical procedures of automatic sorting of resin beads could even be developed.

Experimental Section

The FT-IR mapping was carried out with a Bruker IRScope II instrument. The resin beads modified according to Scheme 1 were embedded in a KBr window under a slight pressure. An area of $3 \times 3 \text{ mm}^2$ was mapped with an IR microscope. With a step width of $50 \mu\text{m}$ 60 data points were measured in the x as well as the y direction, so that a total of 3600 IR spectra were registered for the IR mapping. For a resolution of 4 cm^{-1} and a summation of 4 scans per data point, the measurement time was 5 h.

Received: May 13, 1998 [Z11849IE]

German version: *Angew. Chem.* **1998**, *110*, 3506–3509

Keywords: combinatorial chemistry • IR spectroscopy • microscopy • solid-phase syntheses

- [1] F. Balkenhohl, C. von dem Bussche-Hünnefeld, A. Lansky, C. Zechel, *Angew. Chem.* **1996**, *108*, 2436–2488; *Angew. Chem. Int. Ed. Engl.* **1996**, *35*, 2289–2337.
- [2] J. S. Früchtel, G. Jung, *Angew. Chem.* **1996**, *108*, 19–46; *Angew. Chem. Int. Ed. Engl.* **1996**, *35*, 17–42.
- [3] E. M. Gordon, M. A. Gallop, D. V. Patel, *Acc. Chem. Res.* **1996**, *29*, 144–154.
- [4] *Combinatorial Peptide and Non-peptide Libraries* (Ed.: G. Jung), VCH, Weinheim, **1996**.
- [5] L. A. Thompson, J. A. Ellmann, *Chem. Rev.* **1996**, *96*, 555–600.
- [6] P. H. H. Hermkens, H. C. J. Ottenheijm, D. C. Rees, *Tetrahedron* **1997**, *53*, 5643–5678.
- [7] M. Pursch, G. Schlotterbeck, L.-H. Tseng, K. Albert, W. Rapp, *Angew. Chem.* **1996**, *108*, 3043–3036; *Angew. Chem. Int. Ed. Engl.* **1996**, *35*, 2867–2869.
- [8] S. K. Sarkar, R. Garigipati, J. L. Adams, P. A. Keifer, *J. Am. Chem. Soc.* **1996**, *118*, 2305–2306.
- [9] a) B. Yan, G. Kumaravel, H. Anjaria, A. Wu, R. C. Petter, C. F. Jewell, Jr., J. R. Wareing, *J. Org. Chem.* **1995**, *60*, 5736–5738; b) B. Yan, J. B. Fell, G. Kumaravel, *J. Org. Chem.* **1996**, *61*, 7467–7472.

- [10] B. Yan, G. Kumaravel, *Tetrahedron* **1996**, *52*, 843.
- [11] a) K. Russell, D. C. Cole, F. M. McLaren, D. E. Pivonka, *J. Am. Chem. Soc.* **1996**, *118*, 7941–7945; b) D. E. Pivonka, K. Russell, T. Giero, *Appl. Spectr.* **1996**, *50*, 1471.
- [12] W. J. Haap, D. Kaiser, T. B. Walk, G. Jung, *Tetrahedron* **1998**, *54*, 3705–3724.
- [13] A. Furka, F. Sebestyen, M. Asgedom, G. Dibo, *Int. J. Pept. Protein Res.* **1991**, *37*, 487–493.

Ba₃Ge₄: Polymerization of Zintl Anions in the Solid and Bond Stretching Isomerism**

Fabio Zürcher and Reinhard Nesper*

In memory of Jean Rouxel

In the fast-growing family of Zintl phases, an ever-increasing number of completely new bonding patterns of main group element clusters, Zintl anions, are being discovered. These oligo anions or polyanions often carry relatively high formal charges, which can be determined in accordance with the Zintl–Klemm concept.^[1] In the solid, stabilization is achieved through a large number of surrounding cations. The transfer to solution has only been successful in a few cases until now, most of which were Zintl anions with low formal charges.^[2] It has not yet proved possible to directly dissolve the smaller, highly charged oligomeric anions of Group 14 elements such as E_4^{4-} ,^[3] E_4^{6-} ,^[4] E_8^{16-} ,^[5–7] E_{12}^{21-} ,^[6–8] from the Zintl phase into solution. Apart from E_4 in the form of a tetrahedron^[9] or a butterfly anion, none of these has even been synthesized as a molecular compound.

We investigated the different effects of cations on the Zintl anions in a series of experiments and were able to detect a strong relationship between the polyanion E_n^{m-} formed and the type of cation used. Small, polarizing cations, in particular Mg^{2+} and complex cations such as M_6X^{10+} ($\text{M} = \text{Ca}, \text{Sr}, \text{Ba}$; $\text{X} = \text{O}$) thus favor the formation of highly charged end groups or isolated E^{4-} ions. In contrast, large mononuclear cations preferentially stabilize E–E bonds, whereby the E atoms are less highly charged.^[7] According to the Zintl–Klemm concept, semiconductor structures can only be formed in which the polyanions E_n^{m-} follow the 8– N rule or the cluster counting rules. There are often several structural solutions for a given composition and valence electron number, however, and then the factors mentioned above also play a part in determining the form of the Zintl anion formed. The influence of cation size in determining the structure of the polyanion type for a given electron number has been little investigated

[*] Prof. Dr. R. Nesper, Dr. F. Zürcher
Laboratorium für Anorganische Chemie, ETH Zurich
Universitätsstrasse 6, CH-8092 Zurich (Switzerland)
Fax: + (41) 1-632-1149
E-mail: nesper@inorg.chem.ethz.ch

[**] This work was supported by the Schweizerischen Nationalfonds zur Förderung der wissenschaftlichen Forschung (project no. 20-43228.95).